

Explainable Artificial Intelligence for Sickle Cell Anemia Prediction using Deep Neural Techniques

Bambale Ahmad Salihu¹, Ahmed Aliyu Abubakar², Muhammad Aminu Ahmad³, Murtala Hayatu⁴ and
Halima Lawal⁵

¹Department of Intelligent Computing, Kaduna State University, Kaduna University, Kaduna, Nigeria.

^{2,3}Department of Secure Computing, Kaduna State University, Kaduna University, Kaduna, Nigeria.

^{4,5}Department of Informatics, Kaduna State University, Kaduna University, Kaduna, Nigeria.

as.bambale@kasu.edu.ng¹, ahmed.aliyu@kasu.edu.ng², muhdaminu@kasu.edu.ng³,
murtala.hayatu@kasu.edu.ng⁴, halimalawal32@gmail.com⁵

Abstract

Sickle Cell Disease (SCD) presents substantial diagnostic challenges, and the integration of artificial intelligence (AI) into haematological analysis has the potential to improve early detection and clinical decision-making. However, traditional deep learning models lack transparency, limiting their acceptance in clinical applications. This study aims to develop a transparent and interpretable predictive framework by training a Multilayer Perceptron (MLP) for SCD classification and using an Explainable Boosting Machine (EBM), an inherently interpretable model, to provide post-hoc and global interpretability of the underlying data patterns. This work separates the predictive MLP model from the interpretable EBM model, using the EBM to examine feature importance, trends, and clinical consistency, this method will provide better insight to the predictions made by the MLP Model. A dataset of 50 patient records with 12 haematological features was analysed. The MLP achieved strong predictive performance, and EBM provided clinically aligned explanations, with haemoglobin related biomarkers contributing most strongly to SCD predictions. Evaluation was done, using a confusion matrix and standard performance metrics showed high diagnostic utility while revealing dependent patterns that require clinical caution. The results demonstrate that interpretable models such as EBM can coexist with deep learning to support clinically trustworthy AI. Future work should focus on larger datasets, rigorous external validation, and comparison of emerging XAI techniques to improve diagnostic safety and clinician confidence.

Keywords: Explainable Artificial Intelligence (XAI)₁, Deep Neural Networks (DNN)₂, Multilayer Perceptron Model (MLP)₃, Explainable Boosting Machine (EBM)₄, Sickle Cell Anemia/Disease (SCD)₅.

1. Introduction

Blood circulates throughout the body, delivering oxygen to various organs and tissues of the body. Typically, blood cells are round and can last up to 120 days (Yeruva et al., 2020). Sickle cell anemia is a blood disorder that affects the natural structure of haemoglobin in red blood cells. In this condition, red blood cells become sticky and take on a hard, crescent shape, which usually obstructs blood flow within the body (Yeruva et al., 2020). The lifespan of sickle cells is significantly shorter, ranging from 10 to 20 days. The alteration in haemoglobin can lead to severe pain, tissue damage, and serious health issues, in some cases, potentially resulting in death (Yeruva et al., 2020). Approximately 230,000 children are born with Sickle Cell Disease (SCD) annually in Africa, accounting for nearly 80 percent of the global SCD burden (Williams, 2021). Most infant fatalities due to SCD in Africa occur in West African countries, with Nigeria accounting for approximately 80 percent of these deaths (Beli et al., 2024). Approximately 150,000 children are born with SCD each year in the country, with a prevalence rate of 20 to 30 per 1,000 live births. SCD remains a major public health issue in Nigeria, as an estimated forty million people in the nation carry the sickle cell gene (Beli et al., 2024). Nigeria is the country most severely impacted by sickle cell disease globally. Every year, over 100,000 newborns in the nation die from this serious disorder (Adeniran et al., 2020). Manual evaluation, diagnosis, and cell counting are lengthy procedures that can lead to misclassification and inaccuracies, given that there are millions of red blood cells in a single sample. The rapid advancement of AI technology offers a chance to integrate it into clinical practice, which could transform healthcare services. It is essential to record and share insights about the role of AI in clinical settings to provide healthcare professionals with the knowledge and resources needed for successful application in patient care (Alowais et al., 2023). The growing acceptance of AI across various sectors has led to promising outcomes, enhancing productivity and addressing complex challenges (Sharma et al., 2022). Deep learning (DL), a branch of AI designed to mimic human brain functions, has made substantial contributions to medical science, impacting areas like drug discovery, medical imaging, genome synthesis, and disease diagnosis (Sharma et al., 2022). The increase in DL usage in healthcare can be attributed to the types of data employed in its models, whether pre-existing or specially curated, which significantly influences the model's success rate. DL techniques are utilised to identify diseases, including skin lesions, brain disorders, and chronic conditions such as sickle cell anemia, heart disease, and diabetes (Sharma et al., 2022). Digital transformation has accelerated predictive modelling in healthcare across several domains, including patient deterioration, readmissions, mortality, documentation enhancement, disease detection, end-of-life care, patient flow, and chronic care management. Advances in cloud computing, big data, and the Internet of Things allow us to consolidate data from multiple sources, facilitate large-scale computing

and storage of shared resources, and enable connectivity and data exchange through devices equipped with sensors, software, and other technologies. Additionally, the success of artificial intelligence in various applications has led to the development of numerous autonomous systems and precise predictions that support decision-making processes (Yang, 2022). Predictive modelling in healthcare can be intricate, counterintuitive, and frequently difficult to understand (Yang, 2022). These traits can result in limited acceptance and usefulness of predictive solutions in clinical settings because they are often not transparent. To improve the adoption of predictive solutions in healthcare, it is essential to develop approaches that enhance their explainability. By making models more understandable, we can improve comprehension of their results, increase the practical application of these outputs, and ultimately enhance patient care outcomes (Yang, 2022). Deep Neural Networks have shown promising results in various medical applications, including disease identification. The black-box nature of DNN models hinders their transparency and interpretability, which are crucial in medical diagnoses and will, in turn, build trust among clinicians and patients. Yeruva et al., (2020) introduced a method that addresses the shortcomings of manual research using a sophisticated and effective MLP classification algorithm. This algorithm classifies Sickle Cell Anemia (SCA) into three categories: Normal (N), and Sickle Cells (S) in red blood cells (Yeruva et al., 2020). The opaque nature of the Multilayer Perceptron makes it impossible for users to understand how the prediction was arrived at; therefore, the need for an explainable and interpretable model is evident. AI's application in the medical domain is usually divided into three: Image-based models/frameworks, text-based models/frameworks, and image-text-based models/frameworks. The need for XAI models is to eliminate the black-box nature of non-explainable AI systems in the decision-making process of these models, ensuring that clinicians and patients can understand and trust the predictions made by the model.

2. Related Works

Healthcare is a sector where some applications require clear explanations. Unlike most other fields where the "black box" nature of AI systems can be acceptable, transparency is crucial in healthcare due to potential severe consequences which might result from errors. This research by Koua et al., (2024) presents SCSScreen, a human-guided deep learning system that enhances neonatal screening for sickle cell disease (SCD) by automating the analysis of isoelectric focusing (IEF) images from agarose gels. To overcome the limitations of traditional, error-prone manual interpretation, the system uses convolutional neural networks (CNNs) and introduces a key innovation: an "Unconfirmed" (NC) category for ambiguous cases, which are then re-evaluated by a second-intention model that provides probability scores for each potential SCD profile. Achieving over 98% accuracy in identifying

various SCD types, including major syndromes, and validated with real-world data, SCSScreen offers a robust, cost-effective solution that integrates AI with clinical expertise to improve screening efficiency and healthcare outcomes, particularly in resource-limited settings (Koua et al., 2024). The study by Jennifer et al., (2023) introduces a robust deep learning framework for the automated classification of sickle cell disease (SCD) using microscopic erythrocyte images. To address the limitations posed by the small size of the erythrocytesIDB dataset, the authors apply extensive data augmentation and evaluate five transfer learning architectures ResNet-50, AlexNet, VGG-16, VGG-19, and MobileNet along with a custom CNN model. Each model undergoes hyperparameter optimization, followed by ablation experiments in which traditional fully connected layers are replaced with Support Vector Machine (SVM) and Random Forest (RF) classifiers to assess their individual contributions to overall performance. The findings reveal consistently strong classification results, with the MobileNet–SVM combination achieving the highest accuracy (99.53 %), closely followed by ResNet-50, SVM (99.32 %). Statistical analysis further underscores MobileNet’s significant improvement. Overall, the research demonstrates that integrating transfer learning, systematic hyperparameter tuning, strategic data augmentation, and classifier-level ablation can markedly enhance the reliability and efficiency of automated SCD diagnosis (Jennifer et al., 2023). The article by Singh et al., (2025) proposes a rigorous ensemble-based machine learning framework for the prediction of haemoglobin anaemia using a comprehensive set of 24 haematological markers. Following systematic data preprocessing and feature selection via mutual information, the study evaluates several classification algorithms among them Random Forest, CatBoost, XGBoost, and KNN with the XGBoost and stacked ensemble models attaining the highest predictive accuracy of 99%. To mitigate the opacity commonly associated with machine learning models, the authors employ multiple Explainable AI (XAI) techniques, including SHAP, LIME, ELI5, Anchor, and QLattice. These interpretability methods consistently identify TSD, SD, vitamin B12, folate, and ferritin as the most critical predictors of haemoglobin anaemia. Collectively, the findings demonstrate that integrating optimized ensemble learning with robust XAI methodologies yields a highly accurate and interpretable diagnostic tool, underscoring the potential of data-driven approaches to enhance clinical decision-making and support early detection of anaemia (Dhruva et al., 2024). The study evaluates the application of artificial intelligence for detecting sickle cell disease (SCD) from peripheral blood smear images, addressing diagnostic challenges in resource-limited settings. Using 73 eligible samples, the authors applied three pretrained deep learning models ResNet18, GoogLeNet, and ResNet50—to classify sickled and normal red blood cells, with haemoglobin electrophoresis serving as the diagnostic gold standard. Significant differences in key haematological parameters (Hb, MCV, MCH) were identified between SCD and non-SCD participants. Among the AI models assessed, ResNet50 demonstrated superior performance with an accuracy of 95.9% and

high precision and recall values, outperforming GoogLeNet and ResNet18. The findings highlight AI's potential to enhance screening accuracy, reduce diagnostic turnaround time, and improve accessibility in high-burden regions, although broader validation and infrastructural considerations remain essential for real-world deployment (Singh et al., 2025). Darshan et al., (2025), presents a machine learning (ML) and Explainable Artificial Intelligence (XAI) methodology for the differential diagnosis of Iron Deficiency Anemia (IDA) and Aplastic Anemia (AA). Leveraging a proprietary dataset of 500 patients characterized by 24 haematological parameters, the study implemented data preprocessing and feature selection using Pearson's Correlation and Mutual Information. A comparative analysis of multiple ML classifiers revealed that a customized stacking ensemble model and the Light Gradient Boosting Machine (LGBM) algorithm attained peak diagnostic accuracy of 96%. To ensure translational relevance and model transparency, five distinct XAI techniques SHAP, LIME, Eli5, Qlattice, and Anchor—were deployed to demystify the predictive logic, identifying critical discriminatory markers including platelet count (PLT), procalcitonin (PCT), mean corpuscular volume (MCV), and absolute lymphocyte count (ABS LYMP). The confluence of high-performance ML with multifaceted explainability frameworks facilitates clinically interpretable predictions, positioning this integrated approach as a viable decision-support system for enhancing diagnostic precision in anemia sub-typing (Darshan et al., 2025). The study by De Silva et al., (2025) conducts a comparative evaluation of machine learning models for the preliminary assessment of blood disease risk, employing a clinical dataset comprising haematological parameters from 1,027 patients. Four classification algorithms Logistic Regression, Decision Tree, Random Forest, and XGBoost were implemented, with tree-based ensembles demonstrating optimal performance by achieving perfect classification metrics, including accuracy and F1-scores of 1.00, whereas Logistic Regression attained 91% accuracy. To elucidate the decision-making processes of these opaque model architectures, the study leveraged Explainable AI (XAI) techniques, specifically SHapley Additive exPlanations (SHAP), which identified mean corpuscular volume (MCV), mean corpuscular haemoglobin (MCH), haemoglobin (HBG), and haemoglobin A (HBA) as the predominant features influencing risk stratification. The findings underscore the efficacy of ensemble tree methods as reliable tools for initial diagnostic screening and highlight the critical role of XAI in fostering model transparency and trustworthiness, thereby laying the groundwork for their integration into clinical decision-support systems (De Silva et al., 2025). This study by Goswami et al., (2024) introduces a novel diagnostic framework for sickle cell disease (SCD) that integrates a semi-automated digital microscopy system with advanced deep learning and explainable artificial intelligence (XAI) methodologies. The custom-developed hardware incorporates a programmable XYZ stage to facilitate systematic, high-resolution image acquisition of peripheral blood smears. The captured images are classified using several deep convolutional neural networks including Darknet-19,

ResNet50, and GoogleNet via transfer learning, achieving an average diagnostic accuracy of 97%. To ensure clinical transparency and trust, the model's decision-making process is elucidated using Gradient-weighted Class Activation Mapping (Grad-CAM), delineating the morphologically aberrant regions that contribute to classification. This integrated approach not only automates and standardizes the diagnostic workflow, thereby mitigating the subjectivity and labour intensiveness of traditional microscopy, but also provides a scalable and interpretable tool with significant potential for improving SCD screening in resource-constrained environments (Goswami et al., 2024). Collectively, these studies depict a critical concept in computational haematology, the necessity of merging high diagnostic accuracy with robust model interpretability to foster clinical trust and actionable insights. Most research has consistently demonstrated that while complex machine learning and deep learning models achieve exceptional performance, they rely on post-hoc explanation techniques such as SHAP, LIME, or Grad-CAM to demystify their "black-box" nature. This recurrent theme powerfully justifies the use of inherently interpretable models like the Explainable Boosting Machine (EBM), which is specifically designed for tabular clinical data. An EBM can deliver state of the art accuracy comparable to ensemble or deep learning methods while providing native, exact visualizations of feature contributions, thereby directly addressing the core clinical need for transparent, reliable, and directly interpretable diagnostic aids without requiring secondary explanation tools.

3. Methodology

This paper employed the use of EBM as the interpretable technique to interpret the prediction model of the MLP prediction model.

3.1 Proposed System

This work, enhanced the MLP Prediction Model using an Explainable Boosting Machine to interpret the developed black-box model. Explainable Boosting Machine is a machine learning model, which is also a glass-box model, it is tree-based, similar to decision trees or random forest ML models, and is highly understandable and explainable. EBM's mechanics begin with learning each feature using gradient boosting or bagging, and the procedure is limited to learning one feature at a time at a minimal learning rate. This procedure is repeated several times, resulting in N number of small tree models for each feature. EBM can compute the pairwise interactions between the trees for each feature, improving classification accuracy without compromising explainability. The EBM will be used to explain and interpret the MLP used in the deep neural network for the identification of sickle

cell anemia. In the MLP, an Explainable Bosting Machine serves as the final layer of the network, which is responsible for making the final decision or prediction based on the output of the preceding layers. EBM and DNN serve different purposes and have different strengths, they can be used together to leverage the transparency and interpretability of EBMs while benefiting from the high predictive power of DNNs. This combination can be particularly useful in applications where model transparency and interpretability are essential, or when you need to evaluate and understand the behaviour of complex DNNs. An architecture of the proposed EBM framework to be developed is shown in the figure below

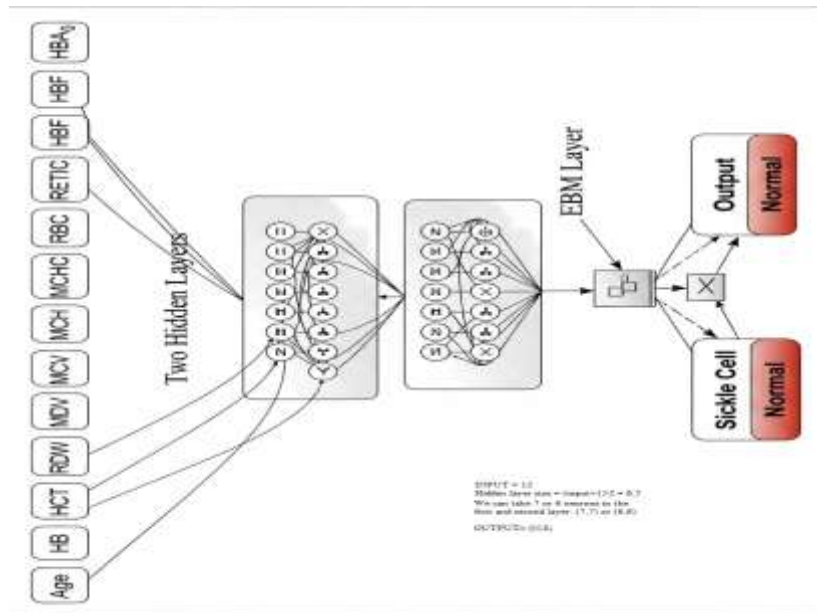


Figure 1: An Architecture of the Proposed EBM Framework

3.2 Dataset

The dataset used for this research consists of 50 records with 12 pre-processed attributes for the prediction of sickle cell anemia. The datasets are

1. AGE (The period that person has lived),
2. Haemoglobin HB (A red protein responsible for transporting Oxygen in the blood of vertebrates.)
3. Haematocrit HCT (The ratio of the volume of red blood cells to the total volume of blood)
4. RBC Distribution Width RDW (It is a measure of the range of variation of red blood cell volume that is reported as part of a standard complete blood count)
5. Mean Corpuscular Volume MCV (It is a measure of the average volume of a blood corpuscle.)

6. Mean Corpuscular Haemoglobin MCH (It is the average mass of haemoglobin per red blood cell in a sample of blood.)
7. Mean Corpuscular Haemoglobin Concentration MCHC (It is a measure of the concentration of haemoglobin in each volume of packed red blood cells.)
8. Red Blood Cell RBC (The blood cells that carry oxygen)
9. Reticulocytes RETIC (An immature red blood cell without a nucleus, having a granular or reticulated appearance when suitably stained.)
10. Foetal Haemoglobin HBF (It is the main oxygen carrier protein in the human foetus.)
11. HBA0 (It is defined as the non-glycated haemoglobin.)
12. HBA2 (It is a normal variant of haemoglobin A that consists of two alpha and two delta chains and are found at low levels in normal human blood).

The dataset that support's this study is available on request. The dataset is not publicly available due to restrictions i.e. their containing information that could compromise the privacy of the patients. Before training the model, data pre-processing steps will be applied, including handling missing values, outlier detection, and feature scaling. Additionally, the dataset will be split into training and testing sets to avoid overfitting and to ensure the generalization of the models.

3.3 Step by Step Outline of the Experimental Setup and Implementation

- I. Dataset Preparation; As previously mentioned, the dataset consists 50 patients record with 12 parameters, which are variables needed to predict a patient being either Normal cell or Sickle cell.
- II. Analysing and Splitting Dataset; the data is classified as AS, NN, SC, SS, ST. The 5 labelled Diagnosis is converted into two main groups. (1) NN = N (Normal Cells) (2) AS, SC, SS, ST = S (Sickle Cells). In machine learning, datasets with multiple labels are categorised in one or more columns. The training data is rendered in words to make it understandable to humans. Label Encoder in python which is a part of Sci-kit Learn Library is used to convert categorical data into numbers (i.e., N-0 and S-1) this is used for understanding predictive model easily. The dataset used was divided into training data and testing data (80 and 20%.) The training dataset contains the target variable which is the output from which the model learns from the features (input data) in order to get a wholesome view of the data.
- III. Developing and training the MLP prediction model
- IV. Applying XAI Technique; Explainable Boosting Machine model was developed to interpret the black box model MLP prediction model.

- V. Model evaluation; The model was evaluated using Accuracy, Precision, Recall (Sensitivity), Specificity, F1-score.
- VI. Result; The result of the explainable model developed and accuracy metrics are presented and explained.

3.4 Predictive Model: Multilayer Perceptron

The MLP classifier was designed using a feedforward architecture with

- I. Input layer: 12 features
- II. Hidden layers: Two layers (64 and 32 neurons)
- III. Activation function: ReLU
- IV. Optimizer: Adam
- V. Loss function: Binary cross-entropy
- VI. Epochs: 100

3.5 Explainable AI Technique Integration

EBM, an inherently interpretable generalized additive model, was trained separately on the same dataset to:

1. Provide global feature importance.
2. Generate feature importance plots.
3. Offer local explanations for predictions.

The EBM is used to explain and interpret the MLP used in the deep neural network for the identification of sickle cell anemia. In the MLP, an Explainable Boosting Machine serves as the final layer of the network, which is responsible for making the final decision or prediction based on the output of the preceding layers. EBM and DNN serve different purposes and have different strengths, they can be used together to leverage the transparency and interpretability of EBMs while benefiting from the high predictive power of DNNs. This combination can be particularly useful in applications where model transparency and interpretability are essential, or when you need to evaluate and understand the behaviour of complex DNNs. This approach ensures transparency without compromising MLP performance.

3.6 Evaluation Method.

The accuracy evaluations of the Multi-layer Perceptron and the Explainable Boosting Machine in the prediction and interpretation of Sickle cell anemia was evaluated with specific focus on datasets. The accuracy performance scores of the interpretability with respect to the dataset was also be presented in the final result. The evaluation was conducted on a separate testing set to ensure unbiased results.

4. Results and discussion

In the following experimental study, the explainability of some candidates of ante-hoc and candidates of post-hoc XAI methods were assessed. In the first phase, the original data sub-sets provided in the benchmark paper were analysed and pre-processed for training the machine learning model (MLP). Secondly, the Machine Learning model was built and optimized on the training sets and used to predict the test sets. Thirdly, the explainability techniques were applied to obtain the explanations and interpretability for the predictions. Finally, the methods of validating the generated explanations were applied.

4.1 Explanation Analysis through Visualization

Feature importance of the dataset

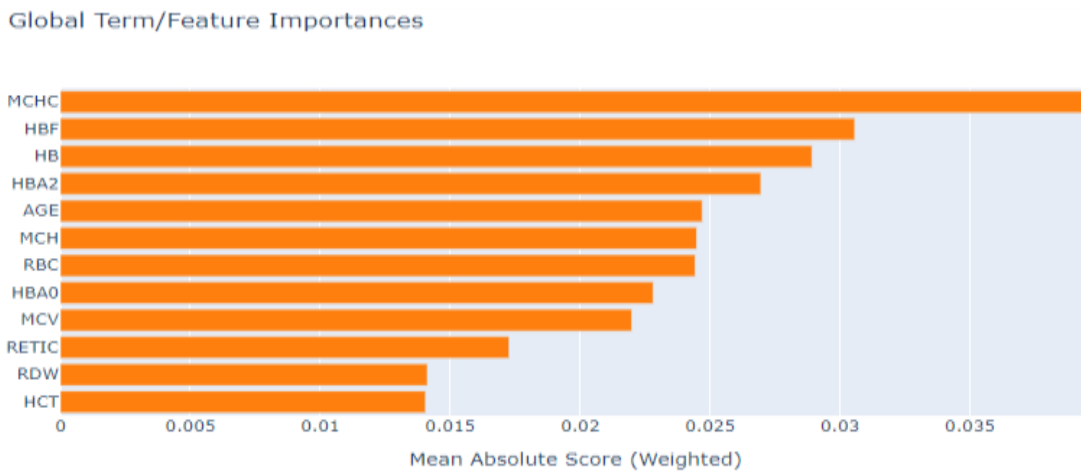


Figure 2: Visualized feature importance mapping of the dataset used in the work.

In Figure 2, the overall features importance of the dataset is shown. This work was done with the explainable boosting classifier global explanation method. Here feature 1(MCHC) is most important, then feature 2(HBF), then feature 3(HB) and then others according to the above figure. Those features are most important to make decisions for the Machine learning algorithm and Explainable Technique. A feature's position on the y-axis determines the EBM'S value position on the x-axis

4.2 Global Feature Explanation for each Attribute.



Figure 3: Analysis of Explainable Boosting Machine (EBM) Feature Term – AGE (Continuous)

Figure 3 represents the AGE feature term from the Explainable Boosting Machine (EBM) model. It shows how age influences the model’s classification among different hematological conditions: Normal and Sickle Cell.

Understanding the Plot Structure

The visualization consists of two parts:

1. **Upper Plot (Score vs. AGE):** Depicts how the EBM model’s score changes with respect to AGE for each class. Y-axis (Score) represents the contribution of AGE to the model’s log-odds (positive values push toward the class, negative values pull away).

Coloured Lines: Represent different classes: **Blue:** Normal and **Green:** Sickle Cell.

2. **Lower Plot (Orange Bars):** Displays the distribution (density) of AGE within the dataset. X-axis (AGE) depicts continuous variable ranging from approximately 5 to 63 years. Taller bars indicate higher sample concentrations at those age ranges.

General Observations

The model’s AGE term remains mostly flat across the entire age range (5–63 years), suggesting that AGE contributes very little to differentiating between classes. Minor fluctuations are observed, but these are relatively small (within ± 0.1 score), indicating weak predictive influence. The AGE

distribution (bottom histogram) shows that most samples are concentrated between 20 and 40 years, with fewer younger (<15) or older (>55) cases.

Interpretation by Class

Normal Class (Blue Line)

The Normal class shows a slight positive bias across most ages, with a near-zero contribution overall with a slight upward movement around ages 40–50 may suggest that mid-age individuals are marginally more likely to be classified as Normal, though the effect is weak.

Sickle Cell Class (Green Line)

The curve remains close to zero or slightly below, implying that age barely influences the prediction of Sickle Cell. Younger individuals (under 20) show slightly more negative scores, possibly reflecting fewer Sickle Cell cases in that range in the training data.

Clinical Interpretation

From a medical perspective, while Sickle Cell disease is often present at birth and diagnosed early in life, patients of all ages are represented in the data due to the chronic nature and ongoing management. Therefore, age alone is insufficient for prediction, aligning with the model’s behaviour. In Normal cases, age distribution overlaps substantially, further reducing its discriminatory power.



Figure 4: Analysis of Explainable Boosting Machine (EBM) Feature Term – HB (Haemoglobin, Continuous)

Figure 4 represents the Haemoglobin (HB) feature term from the Explainable Boosting Machine (EBM) model, showing how variations in HB levels influence predictions across two diagnostic classes: Normal and Sickle Cell. EBM decomposes the model prediction into interpretable feature

effects (scores) for each class label, showing the impact of HB on the classification outcome.

Understanding the Plot

The visualization contains two parts:

1. **Upper Plot (Score vs. HB):** Displays how the model's prediction score changes with different HB values. X-axis (HB) represents Haemoglobin concentration (approx. 6.1–16.5 g/dL).

Coloured Lines: These represents different classes **Blue:** Normal class and **Green:** Sickle Cell class

2. **Lower Plot (Orange Bars):** Shows the distribution of HB values within the dataset (density histogram). Y-axis (Score) Indicates the feature's contribution (log odds) toward a particular class prediction. Taller bars correspond to more samples within that HB range.

General Observations

The EBM response curve for HB shows a distinct pattern indicating meaningful class separation across different HB ranges. With low HB levels (6–10 g/dL), the model leans toward Sickle Cell classification while with moderate HB levels (10–13 g/dL), the model's output is relatively neutral, with minor overlap between Normal and Sickle Cell classes. High HB levels (>13.5 g/dL), the model strongly favours the Normal class.

This pattern aligns with clinical understanding since Sickle Cell patients typically have lower haemoglobin concentrations compared to healthy individuals.

Interpretation by class

Normal Class (Blue Line)

The normal class, shows increasing positive contribution when HB levels exceed 13 g/dL. At low HB values (below 10 g/dL), the contribution drops slightly below zero, reducing the likelihood of classifying the sample as Normal. This behaviour mirrors real-world patterns where healthy individuals typically maintain normal-to-high haemoglobin levels.

Sickle Cell Class (Green Line)

The curve, exhibits negative contributions at higher HB values (>13 g/dL), meaning high haemoglobin levels reduce the model's confidence in predicting Sickle Cell. Between 7–10 g/dL, the curve is slightly positive, showing that low HB values increase the likelihood of classifying as Sickle Cell. The gradual flattening after 11 g/dL indicates diminishing discriminative power in mid-range haemoglobin levels.

Feature Distribution Insights

The dataset is well-represented across HB values from 7 to 15 g/dL, indicating that the model had sufficient samples to learn from. The highest density is observed between 8.7–10.4 g/dL, reflecting the common HB range in Sickle Cell or mild anaemic cases.

Clinical Interpretation

Model logic aligns with haematological norms:

- a. **Low HB** → Anemia → Higher likelihood of **Sickle Cell**.
- b. **High HB** → Normal oxygen-carrying capacity → **Normal classification**.
- c. **Mid-range HB (10–12 g/dL)**: Model shows minimal discrimination, reflecting overlapping patient characteristics.

This shows that HB is a key differentiating feature with clear monotonic behaviour, higher values predict Normal, lower values predict Sickle Cell.

Model Behaviour and Reliability

The nonlinear but smooth transitions confirm that the EBM is not overfitting noise in HB values while the clear separation between Normal and Sickle Cell classes implies strong feature interpretability and medical consistency.

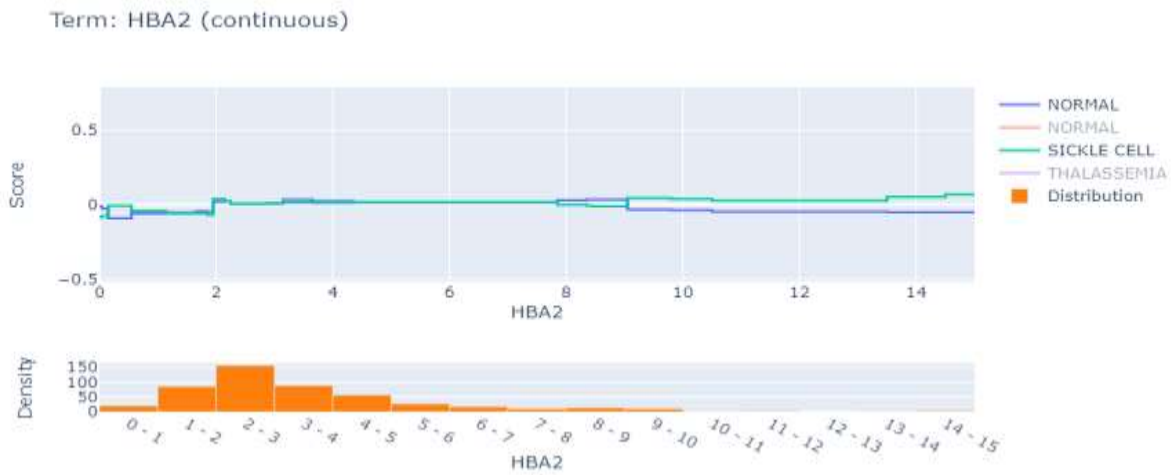


Figure 5: Analysis of Explainable Boosting Machine (EBM) Feature Term – HBA2 (HaemoglobinA2, Continuous)

Figure 5 represents the HaemoglobinA2 (HBA2) feature term from the Explainable Boosting Machine (EBM) model, showing how variations in HBA2 levels influence predictions across two diagnostic classes: Normal and Sickle Cell. It is a normal variant of hemoglobin A that consists of two alpha and two delta chains and are found at low levels in normal human blood. EBM decomposes the model prediction into interpretable feature effects (scores) for each class label, showing the impact of HBA2 on the classification outcome.

Understanding the Plot

The visualization contains two parts:

1. **Upper Plot (Score vs. HBA2):** Displays how the model's prediction score changes with different HBA2 values. X-axis (HbA2), represents Haemoglobin A2 concentration, ranging approximately from 0 to 15.

Coloured Lines: These represent different classes. **Blue:** Normal class and **Green:** Sickle Cell class

2. **Lower Plot (Orange Bars):** Shows the distribution of HBA2 values within the dataset (density histogram). Y-axis (Score), indicates the feature's contribution (log odds) toward a particular class prediction. Taller bars correspond to more samples within that HBA2 range.

Feature: HBA2 (continuous)

- a. **Term Type:** Continuous — this means HBA2 is a numeric variable (e.g., haemoglobin A2 percentage).
- b. **X-axis:** HBA2 values (ranging approximately from 0 to 15).
- c. **Y-axis (top plot):** Model's contribution or **score** for each HBA2 value how much it shifts the prediction towards or away from a specific class.
- d. **Y-axis (bottom plot):** Density or frequency of the HBA2 values across samples.

General Observations

Model's stability across HBA2 displays score lines for all classes (Normal and Sickle Cell) that are flat and close to zero, which means that HBA2 does not have a strong differentiating effect on the prediction. The model sees minimal change in risk or probability for different HBA2 levels. The small deviations in the lines indicate slight model sensitivity at some ranges, but not significant.

Interpretation by class

NORMAL (Blue line):

Nearly constant across the HBA2 range, suggesting HBA2 is not critical for classifying normal individuals.

SICKLE CELL (Green line):

Also flat, but may show slight increases around HBA2 = 8–9, implying minor influence or rare cases with slightly higher HBA2 levels.

All class scores are between -0.5 and $+0.5$, indicating low feature importance for HBA2 in the overall model. EBM assigns a stronger predictive influence to features with larger score variations.

Feature Distribution Insights

Most data points have HBA2 values between 1 and 3, peaking around 2–3, while few samples exist beyond 7, and almost none beyond 10. This skewed distribution implies that the model has limited exposure to high HBA2 values, which can reduce its ability to learn meaningful patterns in those regions (hence the flat effect lines).

The EBM Global Explanations above show how each attribute is responsible for sickle cell anemia with the EBM model trained on weak labelled data

4.3 Local Explanation and Visualization of positive (Sickle cell) and Negative (Normal)

Visualized Local Explanation for some selected prediction (Sickle cell and Normal)

EBM Local Explanation shows which attributes are responsible for sickle cell anemia. The EBM model was trained on strong labelled data.

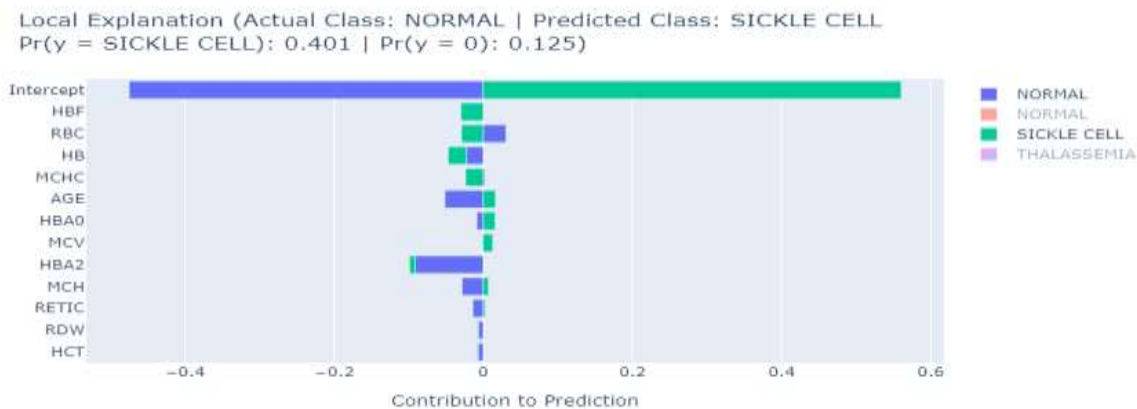


Figure 6: Analysis of Explainable Boosting Machine (EBM) Local Explanation

The visualization presented in Figure 6 represent a local explanation from an Explainable Boosting Machine (EBM) model. It explains how different features contributed to a specific prediction for an individual instance.

Prediction Overview

- I. **Actual Class:** Normal
- II. **Predicted Class:** Sickle Cell
- III. **Model Probabilities:**
 - $\text{Pr}(y = \text{Sickle Cell}) = \mathbf{0.401}$
 - $\text{Pr}(y = \text{Normal}) = \mathbf{0.125}$

The model incorrectly predicted this case as Sickle Cell, even though the true class was Normal. This makes the instance a false positive.

Understanding the Plot

Each bar represents the contribution of a specific feature to the model's final prediction. Features pushing the prediction toward Sickle Cell are shown in green, while those pushing toward Normal are shown in blue. The x-axis measures the contribution magnitude.

Key Feature Contributions

Intercept: The baseline contribution is substantial (around +0.55 toward Sickle Cell). This shows that, before feature adjustment, the model's default bias slightly favours Sickle Cell predictions.

HBF (Haemoglobin F): Contributed positively toward Sickle Cell prediction. Elevated HBF levels are characteristic of some sickle cell variants, explaining this influence.

RBC (Red Blood Cell count): Added a small positive contribution to Sickle Cell classification, possibly indicating slightly lower RBC counts consistent with anemia patterns.

HB (Haemoglobin): Minor positive contribution. Low haemoglobin levels may have influenced the model to lean toward Sickle Cell classification.

AGE: Contributed marginally toward Normal classification, suggesting that age may not align with typical Sickle Cell demographic patterns.

MCV (Mean Corpuscular Volume) & MCHC (Mean Corpuscular Haemoglobin Concentration): These contributed slightly to Sickle Cell prediction. Such indices often differ between normal and anaemic patients.

HBA0, HBA2, HBA2: These haemoglobin fractions had minimal but noticeable effects. HBA2's slight push toward Normal suggests it helps distinguish Normal from thalassaemic or sickle profiles.

RETIC (Reticulocyte count): Very minor contribution, almost neutral. Reticulocyte count is sometimes elevated in sickle cell due to compensatory red cell production.

HCT (Haematocrit): Barely contributed, showing it wasn't a decisive factor for this instance

Interpretation of Model Behaviour

The model overemphasized the baseline and HBF related factors, leading to a false positive classification. The probability difference (0.401 vs. 0.125) is not extreme, suggesting model uncertainty. The prediction is moderately confident but not strong. The bias observation, shows the intercept's high contribution indicates the model might be slightly biased toward predicting Sickle Cell in ambiguous cases.

Clinical and Analytical Implications

Haemoglobin F 's (HBF) strong impact highlights its diagnostic weight but also its potential to cause misclassifications in borderline cases. Balancing feature influence shows recalibration or

regularization may help the model rely less heavily on HBF and the intercept. Feature interaction review suggests that joint effect of RBC, HBF, and HB should be reviewed to understand overlapping signal contributions.

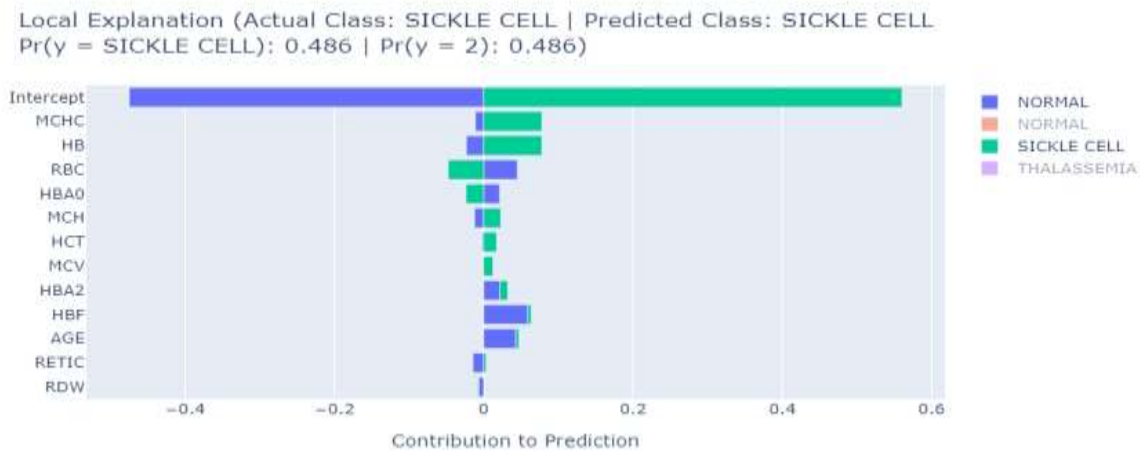


Figure 7 Analysis of Explainable Boosting Machine (EBM) Local Explanation – Correct Prediction Case

The visualization presented in Figure 7 represent a local explanation from an Explainable Boosting Machine (EBM) model for a correctly classified case.

Prediction Overview

- I. **Actual Class:** Sickle Cell
- II. **Predicted Class:** Sickle Cell (Correct Prediction)
- III. **Model Probabilities:**
 - o Pr(y = Sickle Cell) = **0.486**
 - o Pr(y = 2) = **0.486** (Note: depending on label encoding, this also represents Sickle Cell)

This indicates the model correctly recognized the Sickle Cell condition, but with a moderate confidence level (probability 48.6%), suggesting this instance lies near the model’s decision boundary.

Understanding the Plot

Each bar in the plot reflects how much a feature contributes to pushing the prediction toward Sickle Cell (green) or Normal (blue). The x-axis represents the magnitude of contribution to the model’s output.

Key Feature Contributions

Intercept: The largest positive contribution (+0.55), pushing the model strongly toward Sickle Cell classification. This represents the baseline log-odds before individual feature adjustments.

MCHC (Mean Corpuscular Haemoglobin Concentration): Strong positive contribution toward Sickle Cell. This suggests that MCHC values in this instance fall within a range typical of Sickle Cell patients, possibly reflecting higher cell density or altered haemoglobin concentration.

HB (Haemoglobin): Moderate positive contribution. Lower haemoglobin levels are often indicative of Sickle Cell anemia, reinforcing the model's decision.

RBC (Red Blood Cell Count): Shows mixed contribution but slightly positive toward Sickle Cell. RBC counts tend to be lower in sickle patients due to haemolysis, so this aligns with medical expectations.

HBA0 (Haemoglobin A0): Small positive contribution. Reduced levels of HBA0 typically characterize Sickle Cell, which supports the classification.

MCH (Mean Corpuscular Haemoglobin): Slight positive contribution. Reduced MCH often co-occurs with anemia, further confirming the Sickle Cell likelihood.

HCT (Haematocrit): Minimal but positive influence, indicating consistency with Sickle Cell blood composition.

HBA2 and HBF (Haemoglobin Fractions): HBF has a small positive effect, consistent with the known presence of elevated foetal haemoglobin (HBF) in some Sickle Cell patients. HBA2's minimal contribution suggests its level did not strongly influence this instance.

AGE: Negligible contribution, indicating that age did not significantly affect this prediction.

RETIC (Reticulocyte Count): Very small positive effect; this fits since elevated reticulocyte counts often appear in active haemolytic conditions.

RDW (Red Cell Distribution Width): Nearly neutral contribution, showing limited impact on classification.

Interpretation of Model Behaviour

The model's prediction aligns with medical reality, identifying a Sickle Cell case correctly based on blood indices. The dominant influence of MCHC and HB demonstrates that the model is leveraging biologically meaningful indicators of anemia severity. The balanced minor contributions from other haematological features indicate robust model reasoning, without overreliance on a single input. The moderate prediction confidence (0.486) suggests that while the features align with Sickle Cell, their collective evidence was not overwhelmingly strong, possibly due to borderline laboratory values.

Clinical and Analytical Insights

The prediction is consistent with pathology, the feature pattern matches expected physiological trends in Sickle Cell disease. The probability being below 0.5 implies the decision threshold might be near this value. The model’s interpretability shows EBM effectively highlights medically relevant features, supporting trust in its decision.

4.4 Analysis of the Confusion Matrix

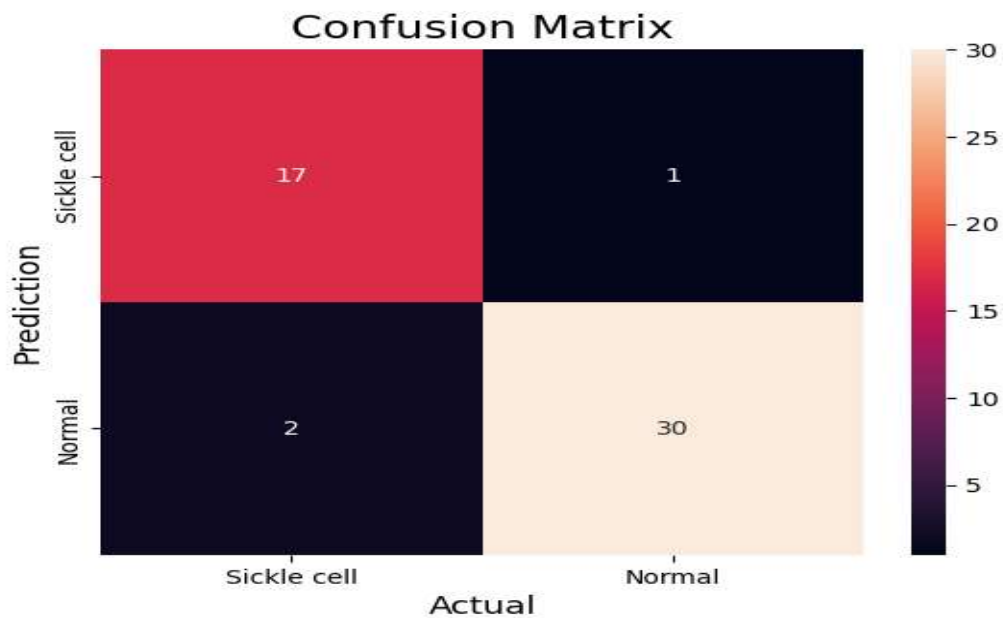


Figure 8: Confusion Matrix

The provided confusion matrix in figure 8 compares predicted and actual classifications for two categories: Sickle cell and Normal. The objective is to evaluate how accurately the model distinguishes between these two classes. The matrix, shows that out of 19 sickle cell cases, the model identified 17 cases correctly as Sickle cell and misclassified 2 as non-sickle cell cases. Similarly, out of 31 non-sickle cell cases, 30 cases were correctly identified as Normal and misclassified 1 as sickle cell. This corresponds with the table 4.1 shown below

| Metric | Accuracy | Precision | Recall | F1 Score | Specificity |
|--------|----------|-----------|--------|----------|-------------|
| Value | 94% | 94.4% | 89.5% | 91.8% | 96.8% |

4.4.1 Performance Metrics

- **Accuracy** = $(TP + TN) / \text{Total} = (17 + 30) / (17 + 1 + 2 + 30) = 47 / 50 = 94\%$
- **Precision (Sickle cell)** = $TP / (TP + FP) = 17 / (17 + 1) = 94.4\%$
- **Recall (Sensitivity)** = $TP / (TP + FN) = 17 / (17 + 2) = 89.5\%$
- **Specificity** = $TN / (TN + FP) = 30 / (30 + 1) = 96.8\%$
- **F1 Score** = $2 * (\text{Precision} * \text{Recall}) / (\text{Precision} + \text{Recall}) = 2 * (0.944 * 0.895) / (0.944 + 0.895) = 91.8\%$

4.4.2 Interpretation

The model performed very well overall (94% accuracy) in distinguishing between Sickle cell and Normal cases, the model also has excellent specificity (96.8%), meaning it rarely misclassifies Normal samples as Sickle cell. The recall (89.5%) suggests a small number of Sickle cell cases are missed 2 out of 19. The precision (94.4%) indicates high reliability when the model predicts Sickle cell. finally, the F1 score (91.8%) balances precision and recall effectively, confirming consistent performance across both metrics.

4.4.3 Error Analysis

1. **False Negatives (2 cases):** These are concerning in medical contexts since missing Sickle cell patients may delay diagnosis or treatment.
2. **False Positives (1 case):** Fewer errors of this kind, but they could lead to unnecessary testing or anxiety.

The model demonstrates strong diagnostic performance with high accuracy and low misclassification rates. However, given the clinical implications, focus should be placed on reducing false negatives to ensure all Sickle cell cases are correctly identified.

5. Conclusion

This study, focuses on the application of explainable artificial intelligence (XAI) to sickle cell anemia prediction using deep neural network models (MLP). The first objective, which is to enhance the MLP prediction model for interpretability and transparency was achieved by developing an EBM model, that serves as the final layer of the MLP prediction model and is responsible for analysing and explaining the importance

and level of contribution of each attribute (feature) of the final prediction. The second objective, which is to evaluate the interpretability and transparency of the result was obtained using confusion matrix, and this was achieved by comparing the predicted and actual classifications for the two categories: Sick cell and Normal. The objective is to evaluate how accurately the model distinguishes between these two classes. However, it is worth noting that the accuracy score of the explainable model is slightly lower than that of the prediction model. This is probably because the complexity of the model increased by adding a separate layer while the basic features were modelled for the explainable structure. Nevertheless, the accuracy in prognosis of both models is acceptable to use for both the defined prediction and explainable problem. In terms of the explanations generated for representative dataset samples, it is interesting to observe the readability of explanations provided by the local technique. To sum up, explanations provided by EBM as bar plots are relatively understandable. EBM includes various types of charts that make it easier to understand a model's prediction when all plotted and studied together. The research on explainable machine learning models is still new but very active and many publications on this topic are published every year. Future research should focus on developing new modelling methods that provide the model's interpretability and maintain the high accuracy of predictions. The use of the attention mechanism will prove to be a promising approach in this topic. Finally, in the future work it would also be interesting to compare the interpretability methods of sickle cell anemia prediction considering other explanation properties such as stability and consistency.

Reference

- Adeniran, A., Oluwole, E. O., & Ojo, O. Y. (2020). The financial burden of sickle cell disease among parents of children with sickle cell disease in Lagos, Nigeria. *International Journal of Scientific Reports*, 6(10), 396. <https://doi.org/10.18203/issn.2454-2156.intjsci20204031>
- Afshar P, Mohammadi A, & Plataniotis KN. (2018). Brain tumor type classification via capsule networks. *IEEE*, 3129–3133.
- Aliyu, H. A., Razak, M. A. A., Sudirman, R., & Ramli, N. (2020). A deep learning alexnet model for classification of red blood cells in sickle cell anemia. *IAES International Journal of Artificial Intelligence*, 9(2), 221–228. <https://doi.org/10.11591/ijai.v9.i2.pp221-228>
- Alom, M. Z., Yakopcic, C., Taha, T. M., & Asari, V. K. (2018). Microscopic Blood Cell Classification Using Inception Recurrent Residual Convolutional Neural Networks. *NAECON 2018 - IEEE National Aerospace and Electronics Conference*, 222–227. <https://doi.org/10.1109/NAECON.2018.8556737>
- Alowais, S. A., Alghamdi, S. S., Alsuhebany, N., Alqahtani, T., Alshaya, A. I., Almohareb, S. N., Aldairem, A., Alrashed, M., Bin Saleh, K., Badreldin, H. A., Al Yami, M. S., Al Harbi, S., & Albekairy, A. M. (2023). Revolutionizing healthcare: the role of artificial intelligence in clinical practice. *BMC Medical*

- Education*, 23(1), 689. <https://doi.org/10.1186/s12909-023-04698-z>
- Alzubaidi Laith and Al-Shamma, O. and F. M. A. and F. L. and Z. J. (2020). Classification of Red Blood Cells in Sickle Cell Anemia Using Deep Convolutional Neural Network. In A. K. and M. P. and G. N. Abraham Ajith and Cherukuri (Ed.), *Intelligent Systems Design and Applications* (pp. 550–559). Springer International Publishing.
- B S, D. D., Sharma, P., Chadaga, K., Sampathila, N., Bairy, G. M., Belurkar, S., Prabhu, S., & K S, S. (2024). An ensemble machine learning framework with explainable artificial intelligence for predicting haemoglobin anaemia considering haematological markers. *Systems Science and Control Engineering*, 12(1). <https://doi.org/10.1080/21642583.2024.2420927>
- Barredo Arrieta, A., Díaz-Rodríguez, N., Del Ser, J., Bennetot, A., Tabik, S., Barbado, A., Garcia, S., Gil-Lopez, S., Molina, D., Benjamins, R., Chatila, R., & Herrera, F. (2020). Explainable Artificial Intelligence (XAI): Concepts, taxonomies, opportunities and challenges toward responsible AI. *Information Fusion*, 58, 82–115. <https://doi.org/https://doi.org/10.1016/j.inffus.2019.12.012>
- Beli, I. I., Ali, L. A., Onuoha, C. C., Jasseh, M., Zentar, M., Belakoul, N., Layadi, Y., Deblui, J. A., Fathi, M., Sani, A. H., Adamu, A. G., Mbahi, M. A., Laachfoubi, T., & Umar, M. (2024). Socio-economic burden of sickle cell disease on families attending sickle cell clinic in Kano state, northwestern Nigeria. *Global Pediatrics*, 9, 100193. <https://doi.org/https://doi.org/10.1016/j.gpeds.2024.100193>
- Bellotti, V., & Edwards, K. (2004). Intelligibility and Accountability: Human Considerations in Context Aware Systems. *Human-Computer Interaction*, 16. https://doi.org/10.1207/S15327051HCI16234_05
- Bobowicz, M., Rygusik, M., Buler, J., Buler, R., Ferlin, M., Kwasigroch, A., Szurowska, E., & Grochowski, M. (2023). Attention-Based Deep Learning System for Classification of Breast Lesions—Multimodal, Weakly Supervised Approach. *Cancers*, 15(10). <https://doi.org/10.3390/cancers15102704>
- Chy, T. S., & Anisur Rahaman, M. (2019). A Comparative Analysis by KNN, SVM & ELM Classification to Detect Sickle Cell Anemia. *2019 International Conference on Robotics, Electrical and Signal Processing Techniques (ICREST)*, 455–459. <https://doi.org/10.1109/ICREST.2019.8644410>
- Damilola Ashorobi, Adam Ramsey, Robert B. Killeen, & Ruchi Bhatt. (2024). Sickle Cell Trait. *National Library of Medicine*.
- Darshan, B. S. D., Sampathila, N., Bairy, G. M., Prabhu, S., Belurkar, S., Chadaga, K., & Nandish, S. (2025). Differential diagnosis of iron deficiency anemia from aplastic anemia using machine learning and explainable Artificial Intelligence utilizing blood attributes. *Scientific Reports*, 15(1). <https://doi.org/10.1038/s41598-024-84120-w>
- David Weatherall. (2011). Inherited Disorders of Hemoglobin. *The Indian Journal of Medical Research*. <https://doi.org/https://pmc.ncbi.nlm.nih.gov/articles/PMC3237249/>
- De Silva, C., & Halloluwa, T. (2025). *Blood Disease Risk Assessment – a Comparative Analysis of Machine Learning Models and XAIbased Model Interpretability*.

- <https://doi.org/10.20944/preprints202503.0808.v1>
- Elsalamony, H. A. (2018). Detection of anaemia disease in human red blood cells using cell signature, neural networks and SVM. *Multimedia Tools and Applications*, 77(12), 15047–15074. <https://doi.org/10.1007/s11042-017-5088-9>
- Encora. (2023). the importance of XAI in healthcare. *Innovation Acceleration. Encora*.
- Gordienko Yu. and Gang, P. and H. J. and Z. W. and K. Yu. and A. O. and R. O. and S. S. (2019). Deep Learning with Lung Segmentation and Bone Shadow Exclusion Techniques for Chest X-Ray Analysis of Lung Cancer. In S. and D. I. and H. M. Hu Zhengbing and Petoukhov (Ed.), *Advances in Computer Science for Engineering and Education* (pp. 638–647). Springer International Publishing.
- Goswami, N. G., Sampathila, N., Bairy, G. M., Goswami, A., Brp Siddarama, D. D., & Belurkar, S. (2024). Explainable Artificial Intelligence and Deep Learning Methods for the Detection of Sickle Cell by Capturing the Digital Images of Blood Smears. *Information (Switzerland)*, 15(7). <https://doi.org/10.3390/info15070403>
- Ibtehaz, N., & Rahman, M. S. (2020). MultiResUNet : Rethinking the U-Net architecture for multimodal biomedical image segmentation. *Neural Networks*, 121, 74–87. <https://doi.org/https://doi.org/10.1016/j.neunet.2019.08.025>
- Ilyas, S., Simonson, A. E., & Asghar, W. (2020). Emerging point-of-care technologies for sickle cell disease diagnostics. *Clinica Chimica Acta*, 501, 85–91. <https://doi.org/https://doi.org/10.1016/j.cca.2019.10.025>
- Jennifer, S. S., Shamim, M. H., Reza, A. W., & Siddique, N. (2023). Sickle cell disease classification using deep learning. *Heliyon*, 9(11). <https://doi.org/10.1016/j.heliyon.2023.e22203>
- Khan, A., Sohail, A., Zahoora, U., & Qureshi, A. S. (2020). A survey of the recent architectures of deep convolutional neural networks. *Artificial Intelligence Review*, 53(8), 5455–5516. <https://doi.org/10.1007/s10462-020-09825-6>
- Koua, K. A. J., Diop, C. T., Diop, L., & Diop, M. (2024). Enhanced neonatal screening for sickle cell disease: Human-guided deep learning with CNN on isoelectric focusing images. *Journal of Infrastructure, Policy and Development*, 8(9). <https://doi.org/10.24294/jipd.v8i9.6121>
- Lei Gao, & Ling Guan. (2023). Interpretability of Machine Learning: Recent Advances and Future Prospects. *IEEE*, 30(4), 105–118.
- Li, L., Wang, Q., & Li, J. (2022). Examining continuance intention of online learning during COVID-19 pandemic: Incorporating the theory of planned behavior into the expectation–confirmation model. *Frontiers in Psychology*, 13. <https://doi.org/10.3389/fpsyg.2022.1046407>
- Malhotra, P., Gupta, S., Koundal, D., Zaguia, A., & Enbeyle, W. (2022). Deep Neural Networks for Medical Image Segmentation. In *Journal of Healthcare Engineering* (Vol. 2022). Hindawi Limited. <https://doi.org/10.1155/2022/9580991>

- National Heart, L. and B. I. (2024). *sickle cell statistics*.
<https://doi.org/https://www.nhlbi.nih.gov/health/sickle-cell-disease>
- Sharma, D. K., Chatterjee, M., Kaur, G., & Vavilala, S. (2022a). 3 - Deep learning applications for disease diagnosis. In D. Gupta, U. Kose, A. Khanna, & V. E. Balas (Eds.), *Deep Learning for Medical Applications with Unique Data* (pp. 31–51). Academic Press.
<https://doi.org/https://doi.org/10.1016/B978-0-12-824145-5.00005-8>
- Sharma, D. K., Chatterjee, M., Kaur, G., & Vavilala, S. (2022b). 3 - Deep learning applications for disease diagnosis. In D. Gupta, U. Kose, A. Khanna, & V. E. Balas (Eds.), *Deep Learning for Medical Applications with Unique Data* (pp. 31–51). Academic Press.
<https://doi.org/https://doi.org/10.1016/B978-0-12-824145-5.00005-8>
- Singh, P., Shah, M., & Dubey, A. K. (2025). Application of Artificial Intelligence in Sickle Cell Identification From Blood Smears: A Potential Game Changer for Developing Nations. *Cureus*.
<https://doi.org/10.7759/cureus.95563>
- Wang, H., Gu, H., Qin, P., & Wang, J. (2020). CheXLocNet: Automatic localization of pneumothorax in chest radiographs using deep convolutional neural networks. *PLOS ONE*, *15*, e0242013.
<https://doi.org/10.1371/journal.pone.0242013>
- Williams, T. N. (2021). Undernutrition: a major but potentially preventable cause of poor outcomes in children living with sickle cell disease in Africa. *BMC Medicine*, *19*(1), 17.
<https://doi.org/10.1186/s12916-020-01892-4>
- World Health Organisation. (2024). *Analytical Fact Sheet Sickle cell disease: the silent killer in Africa Key messages*.
- Wu, W., Liu, G., Liang, K., & Zhou, H. (2021). Pneumothorax Segmentation in Routine Computed Tomography Based on Deep Neural Networks. *2021 4th International Conference on Intelligent Autonomous Systems (ICoIAS)*, 78–83. <https://doi.org/10.1109/ICoIAS53694.2021.00022>
- Yang, C. C. (2022). Explainable Artificial Intelligence for Predictive Modeling in Healthcare. *Journal of Healthcare Informatics Research*, *6*(2), 228–239. <https://doi.org/10.1007/s41666-022-00114-1>
- Yeruva, S., Gowtham, B. P., Chandana, Y. H., Varalakshmi, M. S., & Jain, S. (2021). *Prediction of Anemia Disease Using Classification Methods* (pp. 1–11). https://doi.org/10.1007/978-981-33-4046-6_1
- Yeruva, S., Sharada Varalakshmi, M., Pavan Gowtham, B., Hari Chandana, Y., & Krishna Prasad, P. E. S. N. (2021). Identification of sickle cell anemia using deep neural networks. *Emerging Science Journal*, *5*(2), 200–210. <https://doi.org/10.28991/esj-2021-01270>
- Yeruva, S., Varalakshmi, M. S., Gowtham, B. P., Chandana, Y. H., & Prasad, P. E. S. N. K. (2020). Sickle Cell Disease - A Comprehensive Study and Usage of Technology for Diagnosis. *International Blood Research & Reviews*, 6–14. <https://doi.org/10.9734/ibr/2020/v11i23012>